Journal of Cleaner Production 149 (2017) 60–69

Contents lists available at ScienceDirect

Journal of Cleaner Production

journal homepage: www.elsevier.com/locate/jclepro

Mechanism of solidification of simulated borate liquid wastes with sodium silicate activated slag cements

Nailia R. Rakhimova [a, *], Ravil Z. Rakhimov [a], Vladimir P. Morozov [b], Ludmila I. Potapova [a], Yury N. Osin [c]

[a] Kazan State University of Architecture and Engineering, Kazan, Russian Federation
[b] Kazan Federal University, Kazan, Russian Federation
[c] Interdisciplinary Center for Analytical Microscopy Kazan Federal University, Kazan, Russian Federation

ARTICLE INFO

Article history:
Received 8 November 2016
Received in revised form
18 January 2017
Accepted 8 February 2017
Available online 14 February 2017

Keywords:
Hydration products
Granulated blast furnace slag
Alkali-activated cement
Radioactive waste
Waste management

ABSTRACT

In this study the mineral matrix based on hydrous sodium metasilicate (NSH_5) activated slag cement (AASC) was found to be suitable for solidification of borate solutions with pH 8.5–10.5 and concentration up to 200 g/L. Parameters such as setting times and compressive strength of the waste forms based on AASC and borate wastes can be influenced by the ratio of NSH_5 and H_3BO_3 content. The dosage of 7% Na_2O in the alkali activator per slag provides acceptable setting times and 28-day compressive strength of the waste forms in the range 49.7–56.1 MPa depending on pH of the borate solutions. Lowering the pH of borate solutions results in a reduced rate of setting of the fresh AASC paste, retardation in the structural formation of the hardened AASC paste, a reduced degree of hydration, and a reduction in the amount of calcium silicate hydrates and hydrotalcite. The product of AASC-based mineral matrix and simulated borate wastes interaction is ulexite ($NaCaB_5O_6(OH)_6(H_2O)_5$).

1. Introduction

Progress in nuclear power engineering, with its associated formation and accumulation of nuclear wastes and in conditions of rising requirements for environmental safety, has created an urgent need for the improvement of materials and approaches for reliable immobilization of the wastes (Ojovan, 2011; Shaw and Blundell, 2014). Presently, Portland cement (PC), the most widely used material for solidification of low and intermediate level radioactive wastes (RW), does not always ensure the efficiency of immobilization and accommodation of high load with wastes of diverse composition.

A particular "problematic" waste that results when PC is used as mineral matrix for immobilization is boric acid (H_3BO_3), which is one of the most common types of liquid waste concentrate generated by pressurized water reactors. The main problem in the solidification of boric acid and borate using PC is their strong retarding effect on setting times of the wasteforms (Atabek et al., 1992; Demirbas and Karslioglu, 1995; Le Bescop et al., 1990; Ramachandran and Lowery, 1992). The inhibition effect from the borates often lowers the waste loading needed to obtain qualified solidified waste.

One way to improve the performance of the final wasteforms using cementation technology for "problematic" wastes is to use alternative cements as binders. Alternative cements produce a diverse range of reaction products that, when compared to PC, are characterized by lower solubility and higher ion exchange properties, different pH, faster hardening, and lower permeability of hardened pastes, etc. (Abdel Rahman et al., 2015; Rakhimova et al., 2015; Zhuang et al., 2016; Perna and Hanzlicek, 2014). The differences in composition and structure formation between alternative binders and PC predetermine the differences in the immobilization mechanism. For borate RW, alternative binders such as calcium aluminate, sulphoaluminate, magnesium phosphate, and alkali-activated cements can have higher efficiencies than PC (Champenois et al., 2013, 2015; Qina and Jianlong, 2010; Hall, 2001; Hugo et al., 2015; Yang, 2010; Goni and Guerrero, 2001; Palomo and De la Fuente, 2003; Rakhimova and Rakhimov, 2016).

Previous studies (Palomo and De la Fuente, 2003; Rakhimova and Rakhimov, 2016) have found alkali-activated fly ash and slag cements to be effective in solidifying boron-containing solutions. Experimental results indicated that the leaching indices and

* Corresponding author.
E-mail address: rahimova.07@list.ru (N.R. Rakhimova).

http://dx.doi.org/10.1016/j.jclepro.2017.02.066
0959-6526/

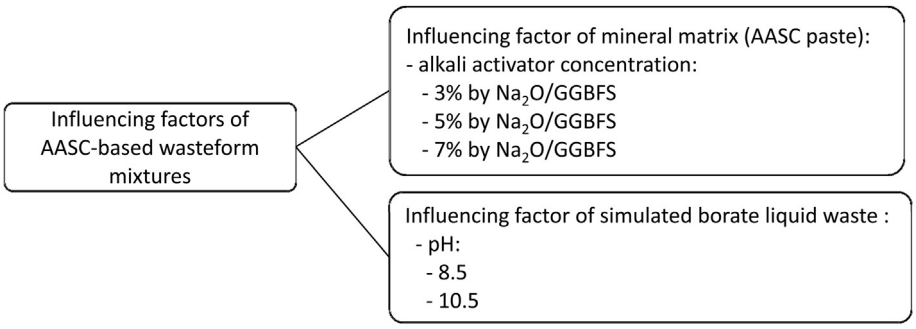

Fig. 1. Influencing factors of AASC-based waste form mixtures.

Table 1
Chemical composition of GBFS.

Component (mass % as oxide)												
SiO_2	CaO	Al_2O_3	MgO	MnO	Fe_2O_3	TiO_2	Na_2O	K_2O	P_2O_5	SO_3	CO_2	LOI
37.49	36.22	11.58	8.61	0.50	0.16	1.80	0.64	0.95	0.01	2.00	–	–

diffusion coefficients of boron in the activated fly ash-based matrix were 100 times lower than those in the Portland cement-based matrix. The authors concluded that the boron present in the alkali-activated fly ash system would precipitate as $NaB(OH)_4$ or other sodium borates, which would fill the voids in the matrix (Palomo and De la Fuente, 2003).

Our results (Rakhimova and Rakhimov, 2016) showed that the ability of NaOH activated slag cement (AASC)to solidify the borate solutions depended on the dosage of the alkali activator NaOH, and the concentrations and pH of the borate solutions. The main reaction products in the 28-day cured system of GGBFS—NaOH—borate solution were C-(A)-S-H, calcite ($CaCO_3$), hydrotalcite $[Mg^{2+}{}_xAl^{3+}{}_y(OH)^-{}_{2(x+y)}(CO_3)^{2-}{}_{y/2}\cdot mH_2O]$, tetrahydroxoborate Na $[B(OH)_4]\cdot 2H_2O$, and ulexite $NaCaB_5O_6(OH)_6\cdot 5H_2O$.

A distinctive feature of alkali-activated cements is that their properties are influenced by many factors including the nature of the alkali activator. Thus, the properties of fresh and hardened alkali-activated slag pastes activated by sodium hydroxide and metasilicate differ. AASC activated by sodium silicate is characterized by higher compressive strength of the hardened paste than that of AASC activated by sodium hydroxide. The drastic difference in C-S-H structure leads to a coarser capillary porosity and to lower compressive strength for the NaOH-activated AASC than for the sodium silicate-activated AASC at the same degree of slag reaction (Ben Haha et al., 2001). Fresh sodium silicate-activated slag pastes are also characterized by short setting times (Andersson and Gram, 1987). This would be a disadvantage in cements intended for building purpose but can be an advantage in solidification of liquid borate RW, which retards the setting of fresh Portland cement pastes.

In this article, the feasibility of the solidification of simulated radioactive liquid borate wastes with sodium metasilicate AASC is investigated. The properties of the fresh and hardened pastes, the hydration products, and the microstructure of the hardened matrices were studied as a function of the dose of the alkali activator and pH of the borate solutions. The dependence of these properties on the factors listed in Fig. 1 is presented in detail.

2. Experimental details

Granulated blast furnace slag (GBFS) obtained from the Magnitogorsky factory was ground in a laboratory planetary mill to a specific surface area (S_{sp}) of 300 m^2/kg (Blaine). The chemical composition of GBFS is shown in Table 1, and the mineralogical composition in Fig. 2. X-ray analysis of GBFS shows that it mainly consists of an amorphous phase and small amounts of gehlenite $Ca_2Al_2SiO_7$ (reflection at 24.036 2θ, PDF 00-035-0755), calcite (reflection at 29.395 2θ,PDF01-071-3699), akermanite $Ca_2(Mg_{0.75}Al_{0.25})(Si_{1.75}Al_{0.25}0_7)$ (reflection at 31.237 2θ, PDF 01-079-2424), hatrurite $Ca_3(SiO)_4$ (reflections at 32.25 and 32.6 2θ, PDF 01-070-8632), stebrodorskite $Ca_2Fe_2O_5$ (reflection at 33.539 2θ, PDF 01-071-2108).

The alkaline activation of the AASC cements was carried out using commercial hydrous sodium metasilicate $Na_2SiO_3\cdot 5H_2O(NSH_5)$. The dosage of $NSH_5$was used to obtain the Na_2O content 3, 5, and 7 %per slag.

Borate solutions designed to simulate real borate radioactive liquid waste produced in a nuclear power plant's pressurized water reactor were prepared by dissolving H_3BO_3 and NaOH in tap water. A control sample was prepared using an equal volume of solution of NSH_5. The concentrations of NaOH, H_3BO_3, and the simulated borate solutions used in the experiments are listed in Table 2.

Cementitious waste samples were prepared by mixing of the borate solutions with a dry mix of GGBFS and NSH_5. A liquid/solid ratio of 0.45 provided a workable and appropriate flowability of the fresh pastes. Vicat' sapparatus was used to measure the setting times in accordance with the method outlined in the EN 196-3 standard (EN 196-3, 1987). The AASC paste samples were prepared in cubic moulds (2 × 2 × 2 cm) for compressive strength tests and then demoulded for 1 day. The cubes were stored for 28 days in sealed plastic bags in a chamber at room temperature and 98% relative humidity; they were also subjected to 90 days of immersion in water before testing. Compression tests were performed by applying a load between the two surfaces that were vertical during casting. Each strength determination quoted is based on the average of six measurements from the same cast.

Calorimetry experiments were carried out using “Thermochron” metering equipment. The pastes were mixed externally, placed in sealed glass ampoules, and loaded into the calorimeter. The time elapsed between the addition of the activating solution to the powder and the loading of the paste into the calorimeter was approximately 3–4 min. The tests were run for 96 h.

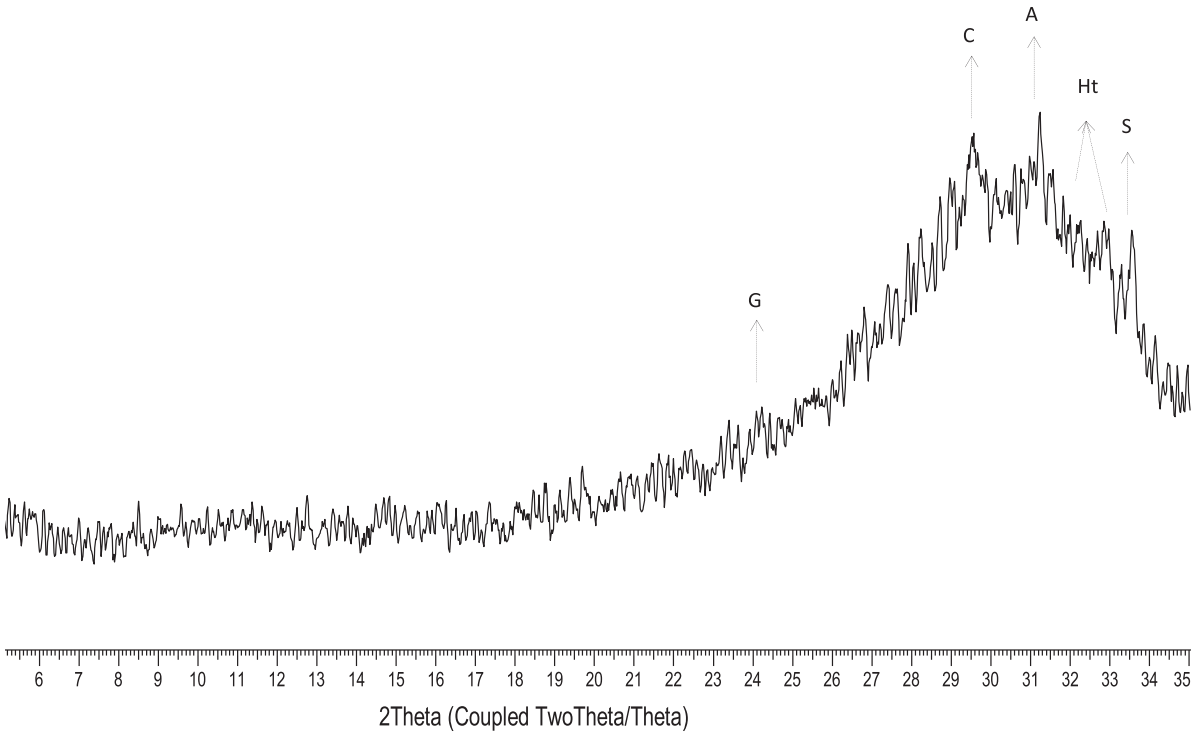

Fig. 2. X-ray diffractogram of GBFS.

Table 2
Composition of prepared simulated borate solutions.

Borate solution	Concentration of NaOH(mol/l)	Concentration of H_3BO_3(mol/l)	Concentration of simulated borate solution(g/L)	pH
Borate solution 1	2.670	0.830	200	8.5
Borate solution 2	2.670	0.420	200	10.5

X-ray diffraction (XRD) and thermal analyses (TG, DTG, DSC) were performed on crushed GBFS and AASC paste samples that had been aged for 28 days. In order to accelerate interaction of AASC paste and borate salts the samples for XRD have been prepared of GGBFS of S_{sp} 300 and 800 m^2/kg. XRD data were collected using a D2 Phaser X-ray diffractometer in a Bragg-Brentano θ–2θ configuration with Cu Kα radiation, operating at 40 kV and 30 mA. The data handling was performed using the DIFFRACplus Evaluation Package – EVA Search/Match and database PDF-2 ICDD. An STA 443 F3 Jupiter simultaneous thermal analysis apparatus was used for TG/DSC. The samples were heated from 30 °C to 1000 °C at a heating rate of 10 °C/min. The data handling was performed using Netzsch Proteus Thermal Analysis.

FTIR spectra were recorded using a Spectrum 65 (Perkin-Elmer) from 4000 to 650 cm^{-1}.

The preparation of fragments of selected samples after 28 days of curing for scanning electron microscopy (SEM, Merlin of CARL ZEISS) observations was done by embedding in epoxy resin, polishing, and carbon coating by (Fig. 3). For qualitative analysis, a set of etalons established in the program Aztec was used (reference standards for X-RAY microanalysis 'Registered Standard No. 8842').

3. Results and discussion

3.1. Properties of fresh and hardened AASC pastes

Tables 3 and 4 show the setting times of the fresh AASC pastes and compressive strengths of the hardened AASC pastes, respectively, made with different concentrations of Na_2O, along with the pH of the simulated borate solutions.

It is well known that the cemented wastes should be allowed to set for more than 5 h to avoid any setting in the mixer in the event of a technical problem, and for less than 24 h to enable good output from the conditioning unit (CauDitCoumes and Courtois, 2003). The results of the current study demonstrate that mixing of AASC with a borate solution slowed the setting process, and that the setting times extended with i) decreasing activator (NSH_5) dose and ii) decreasing pH of the borate solutions. As for the influence of borate solution on the compressive strength of hardened AASC pastes, the compressive strength of AASC mixed with borate solutions is close to or a slightly lower than that of reference samples, with the exception of AASC activated by 3 and 5% Na_2O and mixed with borate solution 1. It should be also noted that the cemented wasteforms demonstrate water resistance and do not substantially lose compressive strength after 3-month immersion tests.

At a Na_2O content of 3%, the AASC is able to solidify borate solution only at pH 10.5, resulting in a 28-day compressive strength of 26.5 MPa of the hardened AASC paste. When the Na_2O content is higher – up to 5 and 7%– all the samples show acceptable setting times, and the compressive strength is up to 56.1 MPa. These results are partially consistent with our previous study (Rakhimova and

Fig. 3. The samples for scanning electron microscopy.

Rakhimov, 2016), but it should be noted that, generally, AASC activated by NSH_5 and mixed with borate solutions demonstrates shorter setting times and higher compressive strength compared to that activated by NaOH.

The results of the calorimetric studies, shown in Fig. 4, are in agreement with the data concerning setting times of the fresh AASC paste.

As can be seen from the data of the calorimetric studies, the increase in activator dosage from 3 to 7% leads to increases in the reaction temperature and peak intensities. The initial peak for the reference formulations, which is attributed to the dissolution of slag particles and the precipitation of a very thin layer of hydration

Table 3
Setting times of fresh AASC pastes along with values for Na_2O%, and pH of the simulated borate solutions.

Na_2O concentration (% by GGBFS)	Mixing solution	Setting times (hour-min)	
		Initial set	Final set
3	water	8–30	23–30
3	borate solution 1	more than 24 h	–
3	borate solution 2	16–00	more than 24 h
5	water	3–35	6–10
5	borate solution 1	9–20	18–30
5	borate solution 2	5–20	14–10
7	water	1–50	3–00
7	borate solution 1	6–20	12–00

Table 4
28-day compressive strength of hardened AASC pastes along with values for Na_2O%, and pH of the simulated borate solutions.

Na_2O concentration (% by GGBFS)	Mixing solution	Compressive strength (MPa)
3	water	29.2
3	borate solution 1	0
3	borate solution 2	26.5
5	water	46
5	borate solution 1	0
5	borate solution 2	44
5*	borate solution 2	38.2
7	water	56.8
7	borate solution 1	49.7
7*	borate solution 1	46
7	borate solution 2	56.1
7*	borate solution 2	54.2

products with a low Ca/Si ratio (Shi and Day, 1996; Brough and Atkinson, 2002), roughly corresponds to the setting times. In comparison with reference sample, for the samples made with borate solutions the peaks corresponding to the beginning of the structure formation process did not coincide with the setting times. In these cases, the peaks were broader and occurred at lower temperatures than in the reference sample. The reason for this mismatch is probably that the setting times were determined not by the formation of the reaction products but by the false set, notably precipitation of borate salts. Actually, 'bulk' reaction products began to form later.

3.2. The influence of borate solutions on the composition of the hydration products and the microstructure of hardened AASC pastes

The matrix formulations, for which the compositions of the hydration products and the microstructures of the hardened AASC pastes were studied, are listed in Table 5.

3.2.1. X-ray diffraction

It is well known that alkali activation of GGBFS results predominantly in the formation of C-(A)-S-H gel (Puertas et al., 2011; Garcia-Lodeiro et al., 2011; Lecomte et al., 2006). This phase is detected as a broad 'hump' by XRD analysis (Fig. 5). The XRD patterns of the AASC1–AASC6 hardened pastes shown in Fig. 5a–c also indicate"relict" GGBFS minerals –gehlenite, akermanite, hatrurite, srebrodolskite. The main reaction products in the 28-day cured system of GGBFS– NSH_5–borate solution are C-(A)-S-H, calcite ($CaCO_3$) (reflection at 29.395 2θ, PDF 01-071-3699), hydrotalcite ($MgO_{6.667}Al_{0.333})(OH)_2(CO_3)_{0.167}(H_2O)_{0.5}$ (reflection at 11.649 2θ, PDF 01-089-0460), calcium silicate hydrate C-S-H (I) $CaO{\cdot}SiO_2{\cdot}H_2O$ (reflection at 7.066 2θ, PDF 00-0034-0002), calcium silicate hydrate C-S-H $Ca_{1.5}{\cdot}SiO_{3.5}{\cdot}H_2O$ (reflection at 29.356 2θ, PDF 00-033-0306), ulexite $NaCaB_5O_6(OH)_6(H_2O)_5$ (reflection at 7.14 2θ, PDF 01-083-1664). Our results are consistent with those of previous studies [16, 25, 35–37] that reported the results of XRD analyses of AASC pastes and sodium borate salts (Abdel Rahman et al., 2015; Ben Haha et al., 2001; Puertas and Fernández-Jiménez, 2003; Wang and Scrivener, 1995). The comparative analysis of XRD patterns of hardened AASCs 1,3, and 5, which are reference samples, shows that increase of Na_2O in systems GGBFS–NSH_5 from 3 to 7 leads to increase of intensities of peaks that are attributed to C-S-H(I) and decrease of intensities of peaks that are attributed to gehlenite and akermanite. As for systems GGBFS–NSH_5 (AASC1, 3, and 5) and GGBFS-NSH_5-borate solution (AASC2, 4, and 6),

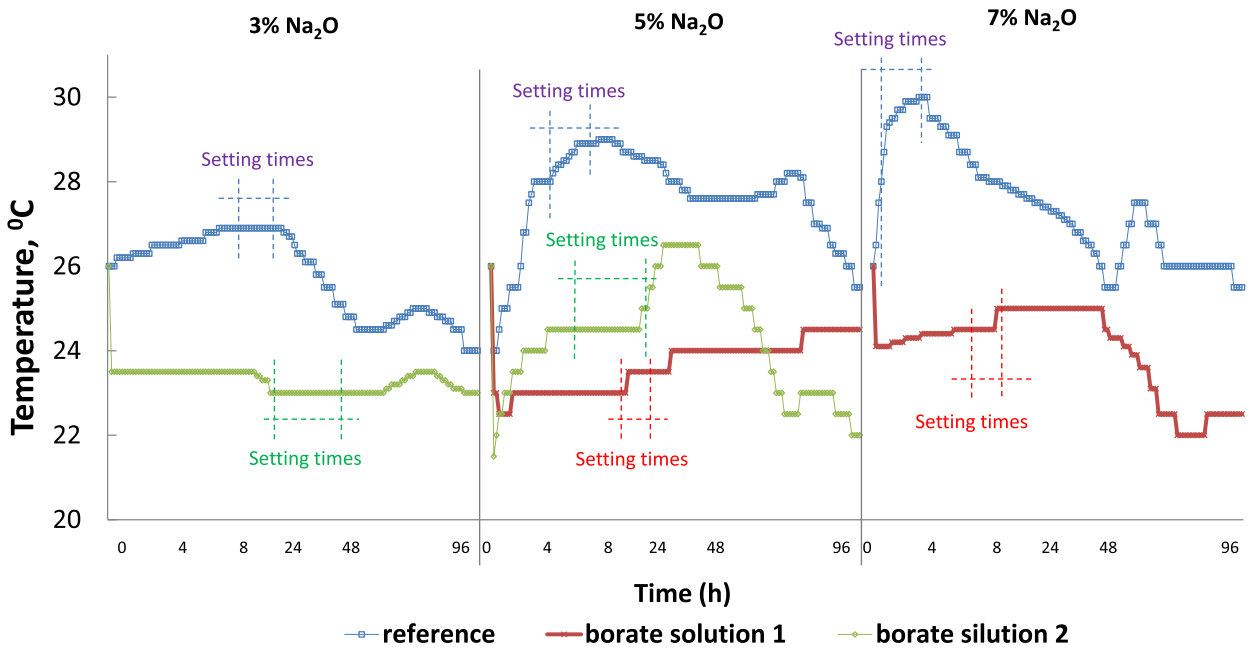

Fig. 4. The hydration rates of fresh AASC pastes, activated by NSH_5 depending on % Na_2O and the pH of mixing solution.

Table 5
The matrix formulations of reference and solidified by simulated borate solutions AASCs.

Abbreviation	Concentration Na_2O (% by GGBFS)	Mixing solution	Ssp of GBFS (m^2/kg)
AASC1	3	water	300
AASC2	3	borate solution 2	300
AASC3	5	water	300
AASC4	5	borate solution 2	300
AASC5	7	water	300
AASC6	7	borate solution 1	300
AASC7	7	borate solution 1	800

comparative analysis shows that the mixing of AASC with borate solutions leads to decrease of intensities of the peaks attributed to C-S-H(I) and hydrotalcite, increase of intensities of the peaks attributed to akermanite, and the appearance of weak peaks of ulexite. Fig. 5d proves the formation of ulexite. As can be seen from Fig. 5d the peaks of ulexite in AASC7 hardened paste are evident and more clear.

3.2.2. TG/DSC

Fig. 6 shows that the reaction products partially observed through XRD are also found in the TG/DSC analyses. It should be also noted the samples AASC2 and 4 based on the GGBFS-NSH_9-nitrate solution are characterized by lower content of bound water than that of reference AASC1 in the range 30–300 °C, which is attributed to calcium silicate hydrates in reference samples and attributed to calcium silicate hydrates.

3.2.3. FTIR

Fig. 7 shows the infrared spectroscopic results for the GGBFS and hardened pastes AASC1–AASC6. An analysis of these spectra confirms the results obtained through XRD and TG/DSC. The signals at 961.67, 954.28, 955.38, 954.14, 955.01, and 962.03 cm^{-1}in samples AASC1-AASC6 are attributed to C-A-S-H-type gel; the signals at 873.16, 873.96, 1413.94, 1414.89, 1457.18, 1418.25, 1430.84, and 1429.56 cm^{-1} are attributed to calcite, which is consistent with previous studies (Fernández-Jiménez et al., 2003; Puertas et al., 2004, 2011; Puertas and Torres-Carrasco, 2014).

The bands at 873.96 and 1414.89 in AASC2 and at 1418.25 and 1429.56 cm^{-1} in samples AASC4 and 6 can be attributed to the asymmetric stretching of B–O in the BO_3 structure, which is consistent with study (Medvedev and Komarevskaya, 2007).

3.2.4. SEM/EDS

Fig. 8 shows an SEM image and EDS results for hardened AASC4 paste. According to the calculation of the Ca/Si ratio for reference samples AASC3 and AASC4 incorporated with borate solution, the Ca/Si ratios were 1.10 ± 0.4 and 1.08 ± 0.6, respectively. Fig. 9 also shows the microstructure of hardened AASC4 paste.

4. Discussion

A comprehensive analysis of the results presented in Section 3 suggests the following sequence of interactions from the mixing of the starting materials to the formation of the hardened pastes in the GGBFS–NSH_5–borate solution system.

Immediately after mixing the constituents of AASC with simulated liquid borate waste, the liquid phase of the fresh paste generally consisted of Na^+cations (from NSH_5 and the borate solution), SiO_3^{2-} and OH^- anions (from NSH_5), Ca^{2+}cations (from GGBFS destruction), and H^+cations and $B(OH)_4^-$ anions (from the borate solution).

The data in Table 3 and Fig. 4 show that a decrease in the pH and alkaline activator NSH_5 retard the setting of the fresh paste. Under these conditions, the temperature of the reaction decreases and the initial peaks are seen after the final setting of the material. Presumably, the retarding effect is caused by following processes in consecutive order:

1) The concentration of OH^- groups, which are essential for destruction of GGBFS, decreases. This decrease is induced by the reaction between H^+ cations from the borate solution and OH^-

groups from the alkaline activator to form H_2O, as well as the reaction of the borate anions with Na^+ to form soluble $NaB(OH)_4 \cdot 2H_2O$. In order to reduce borate-influenced slowing of cement hardening, a process that is based on hydration reactions with water similar to those associated with Portland cement and calcium sulphoaluminate cements, an additional Ca^{2+} source in the form of hydrated lime ($Ca(OH)_2$) is normally used to decrease the slowing influence of borates. Thus, contrary to what is seen in the GGBFS—NSH_5—borate solution system, the alkali activator played roles in both binding the borates and ensuring the hardening of the matrix through activation of GGBFS.

2) Soluble $NaB(OH)_4 \cdot 2H_2O$ can precipitate on the parts of the surface of GGBFS particles, which slows down the rupture of Si-O-Si bonds of GGBFS by OH^- groups. As a result the decreased content of OH^- groups with the introduction of borate solution and partial blocking of the GGBFS particle surfaces by precipitated $NaB(OH)_4 \cdot 2H_2O$ salts slow the rate of structure formation process of the GGBFS-NSH_5-borate solution system. This rate depends on the ratio of the borate solution pH and the concentration of NSH_5. With all this additional alkali activator in the mineral matrix-borate waste system, more OH^- groups are available for interaction with GGBFS and hardening of the wasteforms. The result of this, as can be seen from the XRD and TG/DSC data, is that the influence of borate solutions slows down the formation of Ca-, Si-, Al-, and Mg-containing reaction products like C-S-H(I), C-S-H, and hydrotalcite in hardened AASC pastes mixed with borate solutions compared to reference samples. This hypothesis is also confirmed by the increase of the intensities in the XRD-patterns of the “relict” GBFS minerals gehlenite, akermanite, hatrurite, and srebrodolskite.

Concerning the release of Ca^{2+} from GGBFS in the later stages, the soluble $NaB(OH)_4 \cdot 2H_2O$ reacts with Ca^{2+} to form lesser soluble

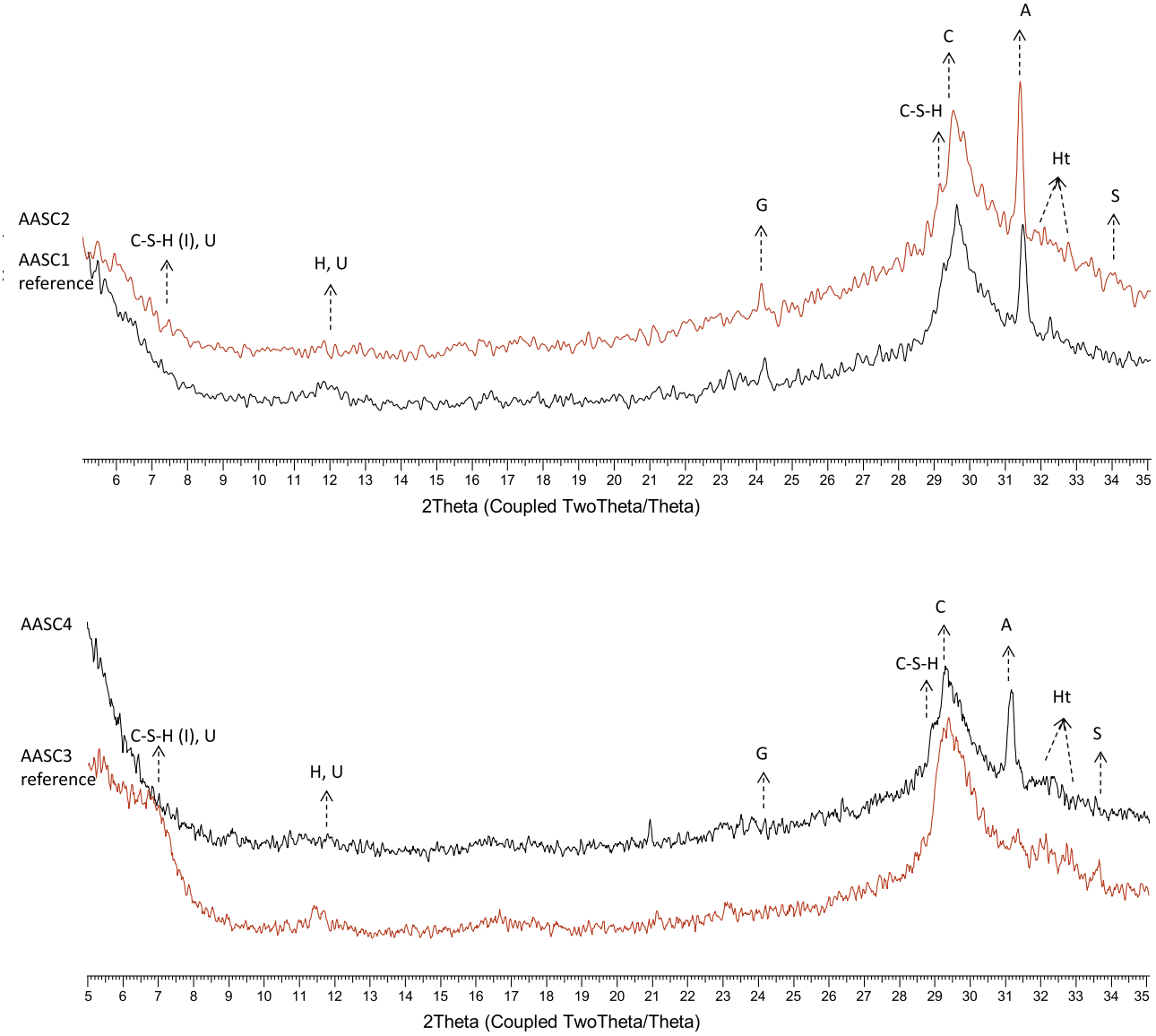

Fig. 5. X-ray diffractograms of hardened AASC pastes: a) AASC1, AASC2; b) AASC3, AASC4; c) AASC5, AASC6; d) AASC7 (C – calcite, G – gehlenite, H – hydrotalcite, C-S-H (I), C-S-H, A – akermanite, Ht – hatrurite, S – stebrodorskite, U – ulexite).

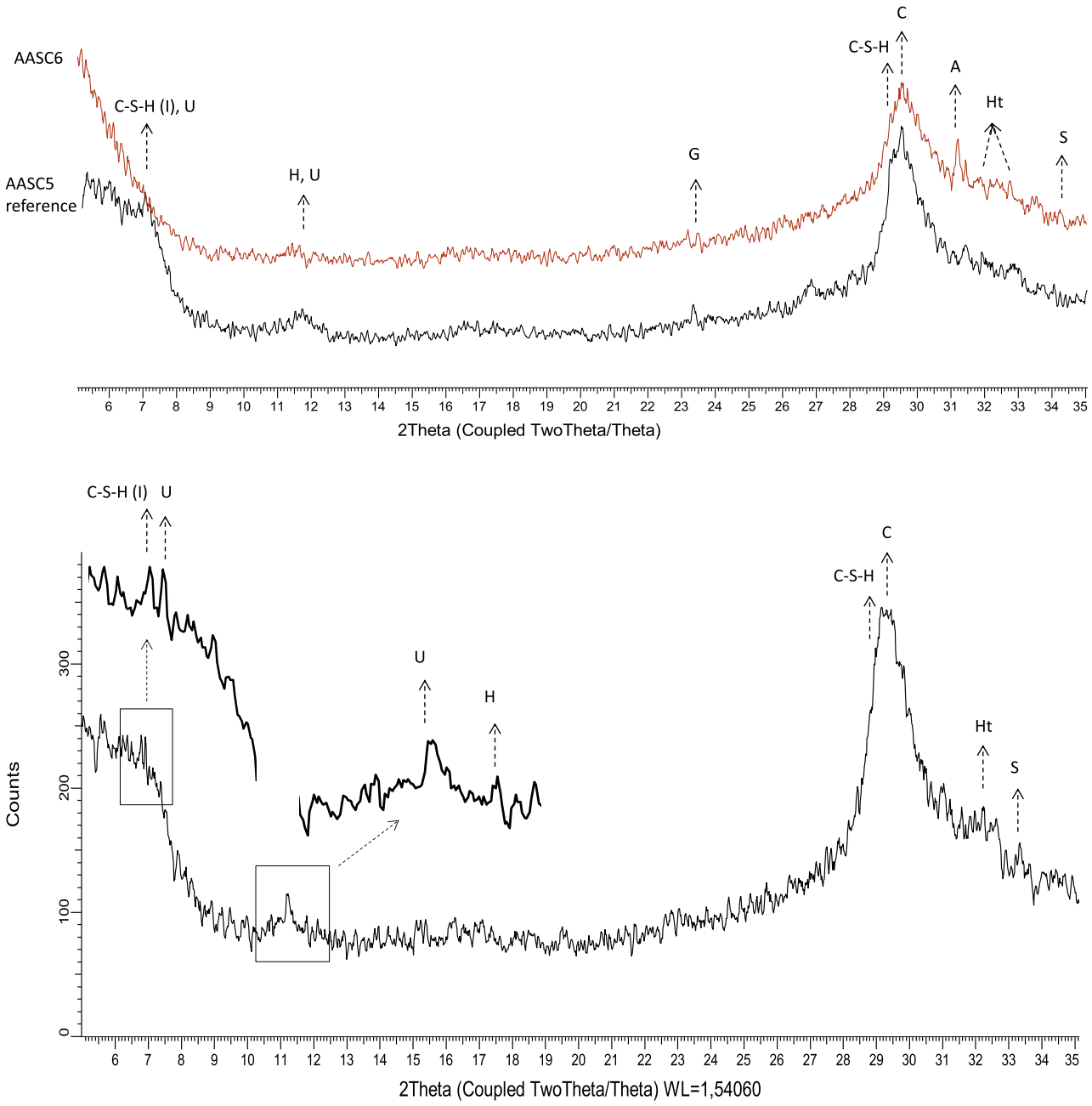

Fig. 5. (*continued*).

reaction products like ulexite ($NaCaB_5O_6(OH)_6(H_2O)_5$), which is partially confirmed by XRD, TG/DSC, and FTIRanalyses.

It should be noted that, despite the lower amount of calcium-silicate-hydrate phases, the mechanical strength of the hardened pastes based on GGBFS–NSH_5–borate solutions was insignificantly lower than that of the reference samples. This is probably because borate salts fill the microcracks and reduce the porosity as can be seen from Fig. 9 and was stated in previous studies on systems based on fly ash-boric acid-calcium hydroxide-sodium hydroxide (Hall, 2001) and using X-ray microtomography on systems based on GGBFS-NaOH-$NaNO_3$ solutions (Ramachandran and Lowery, 1992).

5. Conclusions

In this paper, the feasibility of solidifying borate solutions with concentrations of 200 g/L at pH values of 8.5 and 10.5 with alkali-activated slag was analysed, and the properties of the fresh and hardened pastes, the hydration products, and the microstructure of the solidified waste forms were studied. The following conclusions were reached:

1. The AASC-based mineral matrix was suitable for the efficient solidification of borate solutions with concentrations up to 200 g/L at pH values of 8.5 and 10.5. AASC activated by $NSH_5$with

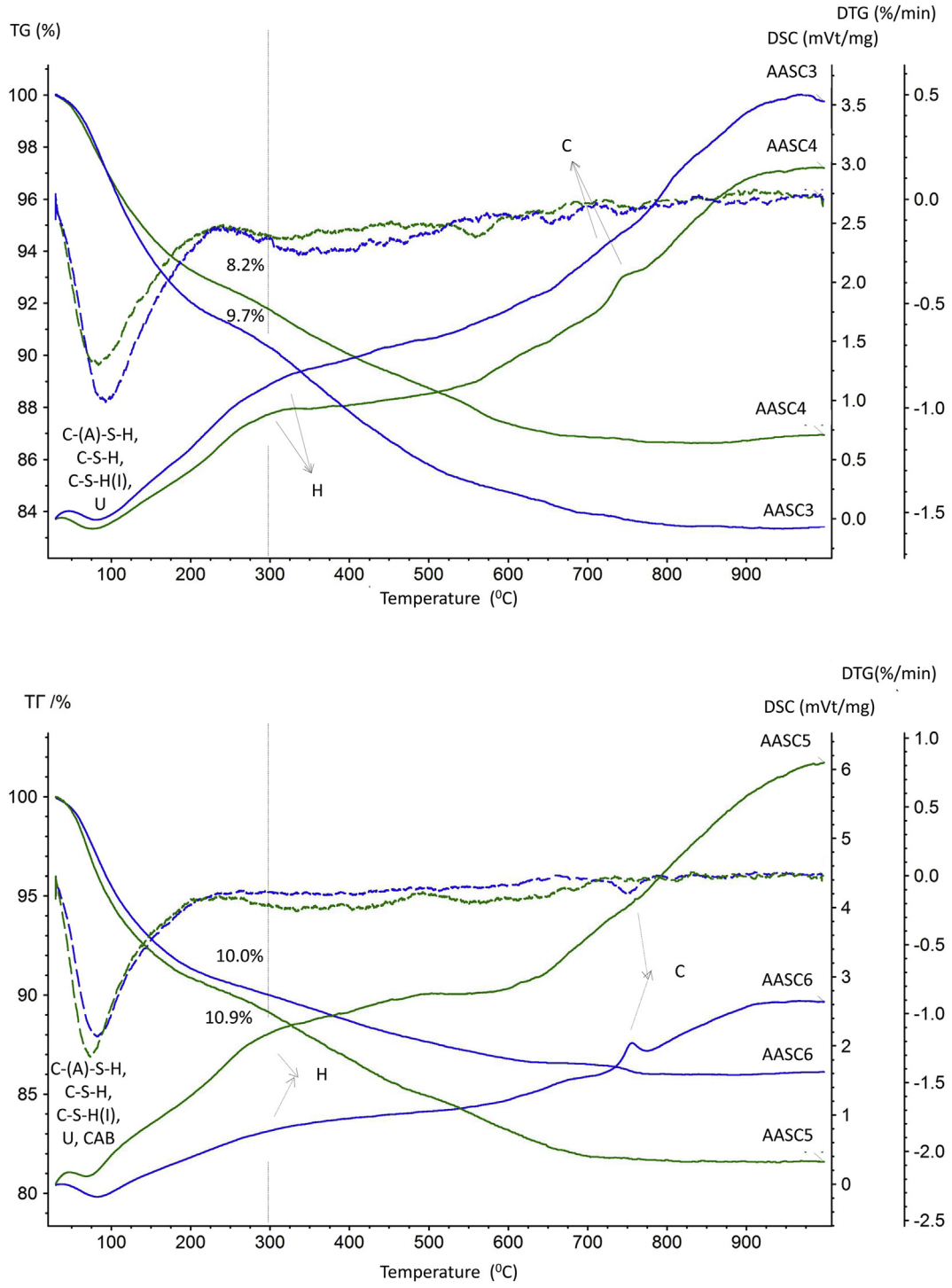

Fig. 6. Thermal analyses (TG/DTG/DSC) of 28-day cured AASC pastes: a) AASC3, 4; b) AASC5, 6.

7% of Na_2O led to acceptable setting times, and the compressive strength of solidified waste forms that had been cured for 28 days was in the range of 49.7–56.1 MPa, depending on the pH of the borate solutions. The compressive strength did not decrease after 3-month immersion tests.

2. The ability of AASC to solidify the borate solutions depended on the dosage of the alkali activator NSH_5 and the pH of the borate solutions. The decreased pH of the borate solutions led to slowing of the setting of the fresh AASC paste, a reduced rate of hydration, and retardation in the structural formation of AASC paste. It also led to lower amounts of calcium silicate hydrates and hydrotalcite. The setting times, compressive strength, and pH of solidifying borate solutions and the increased waste loading can be influenced by the concentration of NSH_5.
3. NaOH plays roles both in binding the borates and in improving the hardening of the matrix through the activation of GGBFS.

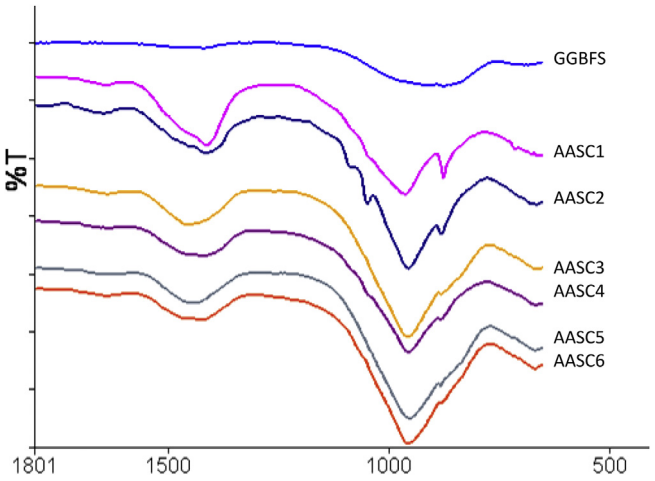

Fig. 7. FTIR spectra of GGBFS powder and AASC1-AASC6.

Studies of fresh and hardened AASC pastes prepared with water and borate solutions have shown that the mechanism by which an AASC-based mineral matrix solidifies borate solutions is based on the precipitation of highly probably $NaB(OH)_4 \cdot 2H_2O$, later ulexite $(NaCaB_5O_6(OH)_6(H_2O)_5)$ following the activation of

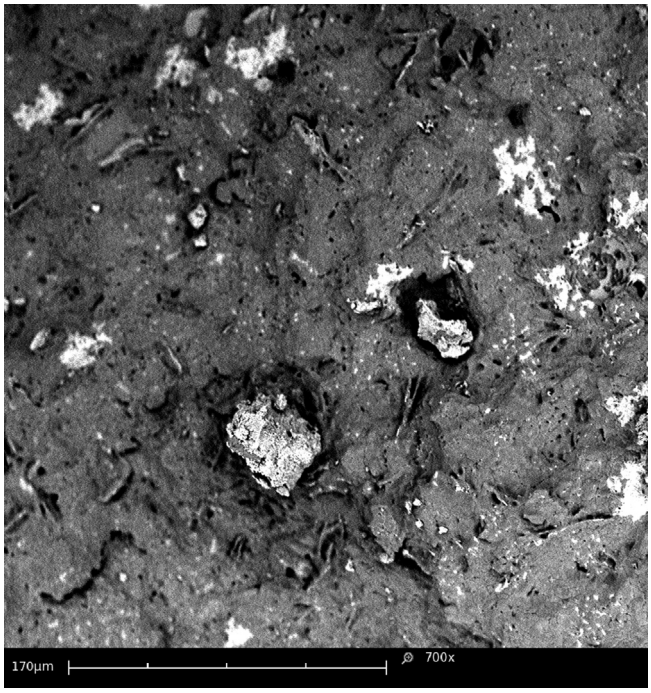

Fig. 9. SEM of hardened AASC4 paste.

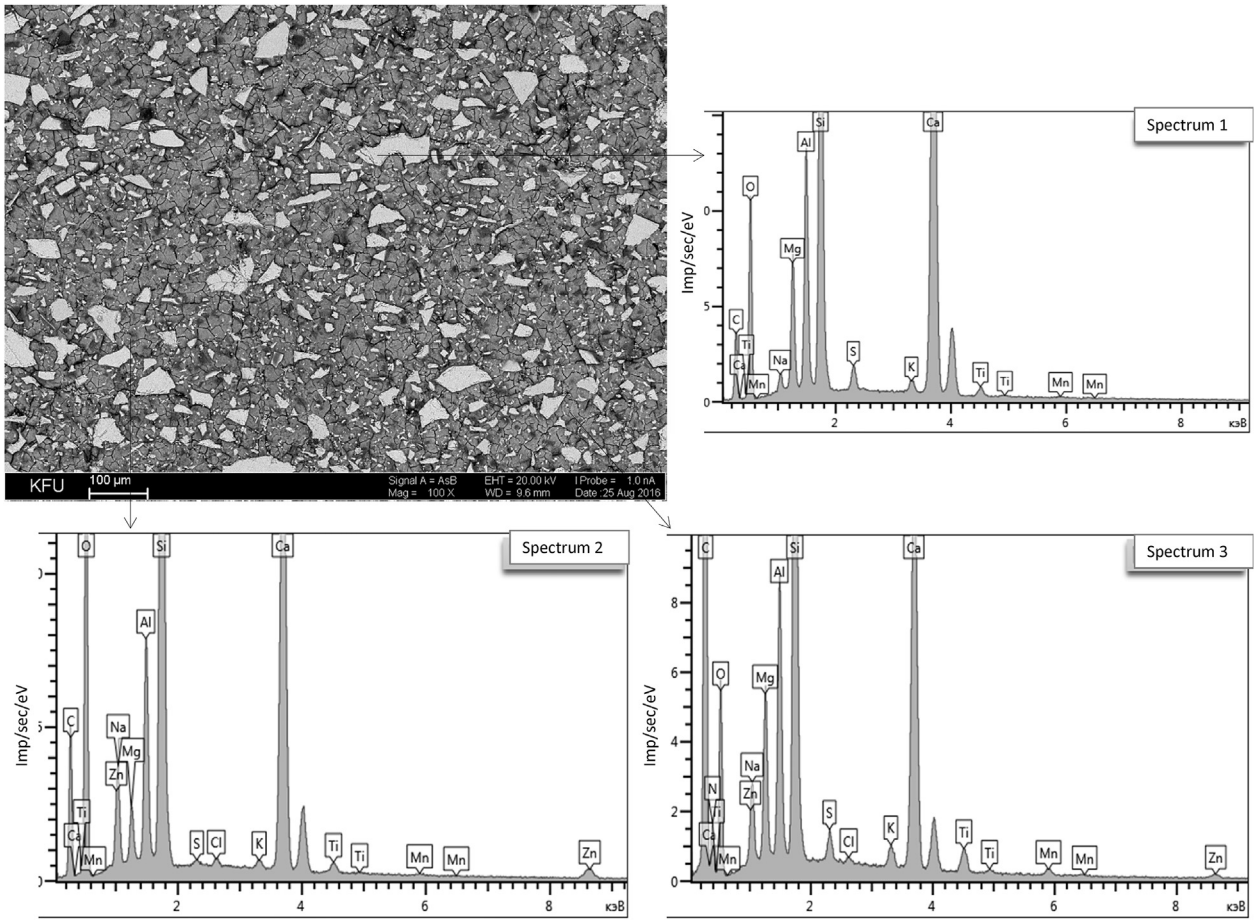

Fig. 8. SEM/EDS of hardened AASC4 paste.

GGBFS with an alkali. The result is the hardening of the AASC-based wasteforms.

References

Abdel Rahman, R.O., Rakhimov, R.Z., Rakhimova, N.R., Ojovan, M.I., 2015. Cementitious Materials for Nuclear Waste Immobilization. Wiley, UK.

Andersson, R., Gram, H.-E., 1987. Properties of alkali-activated slag concrete. Nord. Concr. Res. 6 (1987), 7–18.

Atabek, R., Bouniol, P., Vitorge, P., Le Bescop, P., Hoorelbeke, J.M., 1992. Cement use for radioactive-waste embedding and disposal purposes. Cem. Concr. Res. 22, 419–429.

Ben Haha, M., Le Saout, G., Winnefeld, F., Lothenbach, B., 2001. Influence of activator type on hydration kinetics, hydrate assemblage and microstructural development of alkali activated blast-furnace slags. Cem. Concr. Res. 41, 301–310.

Brough, A.R., Atkinson, A., 2002. Sodium silicate-based, alkali-activated slag mortars Part I. Strength, hydration and microstructure. Cem. Concr. Res. 32, 865–879.

CauDitCoumes, C., Courtois, S., 2003. Cementation of a low-level radioactive waste of complex chemistry: investigation of the combined action of borate, chloride, sulfate and phosphate on cement hydration using response surface methodology. Cem. Concr. Res. 33, 305–316.

Champenois, J.-B., CauDitCoumes, C., Poulesquen, A., Le Bescop, B., Damidot, D., 2013. Conditioning highly concentrated borate solutions with calcium sulfoaluminate cement. In: Bart, F., CauDitCoumes, C., Frizon, F., Lorente, S. (Eds.), Cement-based Materials for Nuclear Waste Storage. Springer, New York, pp. 203–214.

Champenois, J.-B., Dhoury, M., CauDitCoumes, C., Mercier, C., Revel, B., Le Bescop, P., Damidot, D., 2015. Influence of sodium borate on the early age hydration of calcium sulfoaluminate cement. Cem. Concr. Res. 70, 83–93.

Demirbas, A., Karslioglu, S., 1995. The effect of boric acid sludges containing borogypsum on properties of cement. Cem. Concr. Res. 25, 1381–1384.

EN 196-3, 1987. Methods of Testing Cement, Determination of Setting Time and Soundness. European Committee for Standardisation.

Fernández-Jiménez, A., Puertas, F., Sobrados, I., Sanz, J., 2003. Structure of calcium silicate hydrates formed in alkaline-activated slag: influence of the type of alkaline activator. J. Am. Ceram. Soc. 86 (8), 1389–1394.

Garcia-Lodeiro, I., Palomo, A., Fernández-Jiménez, A., Macphee, D.E., 2011. Compatibility studies between N-A-S-H and C-A-S-H gels. Study in the ternary diagram Na_2O–CaO–Al_2O_3–SiO_2–H_2O. Cem. Concr. Res. 41, 923–931.

S. Goni, A. Guerrero, Stability of calcium aluminate cement matrices mixed with borate solution, Conference of Calcium Aluminate Cement, July, 2001, UK.

Hall, D.A., 2001. The effect of retarders on the microstructure and mechanical properties of magnesia–phosphate cement mortar. Cem. Concr. Res. 31, 455–465.

L. Hugo, C. CauDitCoumes, D. Lambertin, C. Cannes, S. Delpech, S. Gauffinet, Influence of boric acid on the hydration of magnesium phosphate cement at an early age, Abstract book of the 14th International Congress on the Chemistry of Cement, October, 2015, Beijing, China.

Le Bescop, P., Bouniol, P., Jorda, M., 1990. Immobilization in cement of ion exchange resins. Mater. Res. Soc. Symp. Proc. 176, 183–189.

Lecomte, I., Henrist, C., Liégeois, M., Maseri, F., Rulmont, A., Cloots, R., 2006. (Micro)-structural comparison between geopolymers, alkali-activated slag cement and Portland cement. J. Eur. Ceram. Soc. 26, 3789–3797.

Medvedev, E.F., Komarevskaya, A., 2007. IR spectroscopic study of the phase composition of boric acid as a component of glass batch. Glass Ceram. 64, 42–46.

Ojovan, M.I., 2011. Handbook of Advanced Radioactive Waste Conditioning Technologies. Woodhead Publishing, USA.

Palomo, A., De la Fuente, J.I., 2003. Alkali-activated cementitious materials: alternative matrices for the immobilisation of hazardous wastes, part I. Stabilisation of boron. Cem. Concr. Res. 33 (2), 281–288.

Perna, I., Hanzlicek, T., 2014. The solidification of aluminium production waste in geopolymer matrix. J. Clean. Prod. 84 (12), 657–662.

Puertas, F., Fernández-Jiménez, A., 2003. Mineralogical and microstructural characterization of alkali-activated fly ash/slag pastes. Cem. Concr. Comp. 25, 287–292.

Puertas, F., Torres-Carrasco, M., 2014. Use of glass waste as an activator in the preparation of alkali-activated slag. Mechanical strength and paste characterisation. Cem. Concr. Res. 57, 95–104.

Puertas, F., Fernández-Jiménez, A., Blanco-Varela, M.T., 2004. Pore solution in alkali-activated slag cements pastes. Relation to the composition and structure of calcium silicate hydrate. Cem. Concr. Res. 34, 139–148.

Puertas, F., Palacios, M., Manzano, H., Dolado, J.S., Rico, A., Rodríguez, J., 2011. A model for the C-A-S-H gel formed in alkali-activated slag cements. J. Eur. Ceram. Soc. 31, 2043–2056.

Qina, S., Jianlong, W., 2010. Cementation of radioactive borate liquid waste produced in pressurized water reactors. Nucl. Eng. Des. 240, 3660–3664.

Rakhimova, N.R., Rakhimov, R.Z., 2016. Mechanism of solidification of simulated borate wastes by sodium hydroxide activated slag cement. Cem. Appl. 4, 96–99 (in Russian).

Rakhimova, N.R., Rakhimov, R.Z., Osin, Y.N., Naumkina, N.I., Gubaidullina, A.M., Yakovlev, G.I., Shaybadullina, A.V., 2015. Solidification of nitrate solutions with alkali-activated slag and slag–metakaolin cements. J. Nucl. Mater 457, 186–195.

Ramachandran, V.S., Lowery, M.S., 1992. Conduction calorimetric investigation of the effect of retarders on the hydration of Portland cement. Thermochim. Acta 195, 373–387.

Shaw, D., Blundell, N., 2014. Analysing causes of avoidable waste in complex systems: a case study from the nuclear industry. J. Clean. Prod. 85 (12), 41–50.

Shi, C., Day, R.L., 1996. A calorimetric study of early hydration of alkali-slag cements. Cem. Concr. Res. 25 (6), 1333–1346.

Wang, S.-D., Scrivener, K.L., 1995. Hydration products of alkali activated slag cement. Cem. Concr. Res. 25, 561–571.

Yang, J., 2010. Effect of borax on hydration and hardening properties of magnesium and potassium phosphate cement pastes. J. Wuhan. Univ. Techn. Mater. Sc. Ed. 25, 613–618.

Zhuang, X.Y., Chen, L., Komarneni, S., Zhou, C.H., Tong, D.S., Yang, H.M., Yu, W.H., Wang, H., 2016. Fly ash-based geopolymer: clean production, properties and applications. J. Clean. Prod. 125 (7), 253–267.